"Hairy Surface Layer" Concept of Electrophoresis Combined with Local Fixed Surface Charge Density Isotherms: Application to Human Erythrocyte Electrophoretic Fingerprinting

ARTICLE *in* LANGMUIR · OCTOBER 1996

Impact Factor: 4.46 · DOI: 10.1021/la960204m

4 AUTHORS, INCLUDING:

Hans Bäumler
Charité Universitätsmedizin Berlin
91 PUBLICATIONS **2,182** CITATIONS

"Hairy Surface Layer" Concept of Electrophoresis Combined with Local Fixed Surface Charge Density Isotherms: Application to Human Erythrocyte Electrophoretic Fingerprinting

E. Donath

Humboldt Universität Berlin, FB Biophysik, FRG

A. Budde* and E. Knippel

Universität Rostock, Klinik für Innere Medizin, Rostock, FRG

H. Bäumler

Humboldt Universität Berlin, Charité, FRG

Received March 6, 1996. In Final Form: July 2, 1996[⊗]

In order to describe the electrophoretic behavior of "hairy-layer"-coated particles, local charge density isotherms have been combined with considerations of hydrodynamic flow penetration into the layer. An iterative numerical procedure was employed to calculate the electrophoretic mobility as a function of both pH and salt concentration. A major result is that information can be gained regarding the distribution functions of oppositely charged groups from the behavior of the point of zero mobility as a function of pH and salt concentration. The theoretical results were used to reinterprete the electrophoretic behavior of native, neuraminidase-treated and glutaraldehyde-treated human erythrocytes. Theoretical analysis of the experimental data revealed that negative groups had occurred preferentially in the outer regions of the layer. A penetration depth of 1 nm into the 3.5 nm thick hairy layer successfully accounted for the erythrocyte mobility data for all methods of analysis tried. Upon sialic acid removal, alterations of the glycocalyx structure occurred, resulting in possible changes in the fixed charge distribution. It was concluded that intramolecular, as well as intermolecular, electrostatic interactions are important for the structure of the hairy surface layer (glycocalyx). No evidence for the adsorption of small ions was found.

Introduction

As the result of a number of recent theoretical and experimental developments, particle electrophoresis is becoming an increasingly more precise and effective method to explore the surface electrostatic properties of a variety of colloidal and biological particles. Nevertheless, many aspects of electrophoretic behavior are still not completely understood, in particular when there is a complex distribution of the fixed charges at the particle solution interface. The fixed charges, for example, can form a charged layer with electrophoretic properties which cannot be described using the classical Smoluchowski electrophoretic theory. Both the electrostatic and the hydrodynamic interfacial properties differ significantly from those of smooth surfaces where the fixed charges are assumed to be homogeneously distributed in a plane. The development of an appropriate electrophoretic theory which takes into account more realistic cases of fixed charge distributions has been of increasing interest recently. Theoretical descriptions have been developed to describe the case of a charged layer penetrable for hydrodynamic flow.[1−14] These approaches have already been successfully applied to several classes of "hairy layer" particles, such as biological cells, polymer micelles, and microgels.[15−19]

However, to our knowledge, the available theoretical framework for charged surface layers, as far as electrophoresis is concerned, has not been developed for those cases when the fixed charge density is not constant but depends either on pH or ion concentration. This is because the relevant local surface charge density isotherms have been not fully included. Such treatments require numerical rather than analytical solutions. Such a numerical integration has been performed to derive the electric potential profile across a charged hairy layer as a function of pH and salt concentration.[20]

With regard to interpretation of electrophoretic mobility data, emphasis to date has largely centered on describing theoretically the ionic strength dependence of the electrophoretic mobility. This is because changing the ion concentration varies the Debye length, effectively probing the fixed charges at different depths of the charged surface layer.

* E-mail: axel.budde@medizin.uni-rostock.de.

[⊗] Abstract published in *Advance ACS Abstracts,* September 1, 1996.

(1) Pastushenko, V.; Donath, E. *Stud. Biophys.* **1976**, *56*, 7.
(2) Donath, E.; Pastushenko, V. *Bioelectrochem. Bioenerg.* **1979**, *6*, 543.
(3) Jones, I. S. *J. Colloid Interface Sci.* **1979**, *68*, 451.
(4) Wunderlich, R. W. *J. Colloid Interface Sci.* **1982**, *88*, 385.
(5) Levine, S.; Levine, M.; Sharp, K. A.; Brooks, D. E. *Biophys. J.* **1983**, *42*, 127.
(6) Snabre, P.; Mills, P. *Colloid Polym. Sci.* **1985**, *263*, 494.
(7) Jaroshchuk, A. E. *Colloid J.* **1985**, *47*, 369.
(8) Sharp, K. A.; Brooks, D. E. *Biophys. J.* **1985**, *47*, 563.
(9) Donath, E.; Voigt, A. *J. Colloid Interface Sci.* **1986**, *109* (1), 122.
(10) Donath, E.; Voigt, A. *Biophys. J.* **1986**, *49*, 493.
(11) Ohshima, H.; Kondo, T. *J. Colloid Interface Sci.* **1987**, *116*, 305.
(12) Starov, V. M.; Solomentsev, Y. E. *J. Colloid Interface Sci.* **1993**, *158*, 159.
(13) Starov, V. M.; Solomentsev, Y. E. *J. Colloid Interface Sci.* **1993**, *158*, 166.
(14) Ohshima, H. *Adv. Colloid Interface Sci.* **1995**, *62*, 189.
(15) Donath, E.; Lerche, D. *Bioelectrochem. Bioenerg.* **1980**, *7*, 41.
(16) McDaniel, R. V.; McLaughlin, A.; Winiski, A. P.; Eisenberg, M.; McLaughlin, S. *Biochemistry* **1984**, *23*, 4618.
(17) Holt, C.; Dalgleish, D. G. *J. Colloid Interface Sci.* **1986**, *114*, 513.
(18) McLaughlin, S. *Annu. Rev. Biophys. Biophys. Chem.* **1989**, *18*, 113.
(19) Ohshima, H.; Makino, K.; Kato, T.; Fujimoto, K.; Kondo, T.; Kawaguchi, H. *J. Colloid Interface Sci.* **1993**, *159*, 512.
(20) Schnitzer, J. E. *Yale J. Biol. Med.* **1988**, *61*, 427.

S0743-7463(96)00204-1 CCC: $12.00

However, in practice, many experiments are performed as a function of pH. In this way the nature and behavior of the surface groups creating the fixed charge (by dissociation or association) mechanisms can be established. Most interesting in this connection is the question of how the p*K* of a surface-attached group depends on the local environment. Another important issue is the dynamical behavior of the surface charged layer. For example, polyelectrolyte layers change their structure and extension upon changing the ionic conditions.[21−23] The electrostatic behavior of polyelectrolyte layers has recently met growing interest in systems with directed, layer-by-layer buildup of ultrathin, charged multilayer films.[24,25] Two indirect approaches which have been used to study the electrostatics of such polyelectrolyte layers are the use of a pH-dependent flourescent probe[26] and the measurement of surface forces as a function of the electrolyte concentration.[27,28]

The application of appropriate electrokinetic techniques to investigate the structure and dynamics of charged surface layers is rare, despite their potential to provide comprehensive information about electrostatic *and* hydrodynamic properties. One of the reasons for this shortcoming has probably been the exclusion of the *mechanism* of fixed charge generation from the hairy layer electrokinetic theories. To this end we have added a numerical procedure to the charged layer electrophoretic concept, which takes into account the additional (indirect) dependence of the surface charge density on the electric potential provided by the shift of the local pH as compared to the bulk pH. In a charged layer this pH shift depends on the distance from the surface, thus producing a position-dependent apparent p*K*. This is the basic difference from the classic case of a planar surface layered charge.

If anionic and cationic sites are present, the particle may observe a point of zero electrophoretic mobility which usually does not coincide with the point of zero net surface charge density. It is obvious that the *distribution* of the various sites is responsible for this discrepancy. The contribution of the fixed surface charges, located at different distances from the particle surface, to the electrophoretic mobility is basically controlled by the Debye length. For example, if the Debye length is much smaller than the extension of the charged surface layer perpendicular to the surface, and also the layer friction coefficient for hydrodynamic flow is large, then it is obvious that only the outermost fixed charges contribute to the mobility. If flow through the layer is possible, then more deeply located fixed charges also, although to a lesser extent, determine the electrophoretic mobility. Hence, varying the Debye length in connection with electrophoretic investigations can provide valuable information on the spatial distribution of the fixed charges. Consequently, a combined variation of ionic strength and pH is thus necessary for a comprehensive electrophoretic investigation. To underline the significance of the resulting three-dimensional graph for the characterization of the surface structure, this method has been called "electrophoretic fingerprinting".[29,30]

One of the biological particles which is studied most often in electrophoresis is the human erythrocyte.[31−34] Despite these studies, several aspects of the electrophoretic mobility behavior, e.g. the dependence of the zero point of mobility on the pH, are still not completely understood. It is widely accepted that the receptor properties of human red blood cells, as well as other cells, depend on salt concentration and pH.[35,36] Standard antigen−antibody tests in clinical diagnosis take into account these dependencies, although the physicochemical background has not been quantified.[37,38] It is quite certain that the surface layer structure and its dynamic response to a change of electrostatic conditions are responsible for these interesting features of the cell surface. An advantage of using the human erythrocyte as a model colloid particle to study hairy layer effects is that many aspects of the chemical composition and the structure of the surface layer are known. Therefore, we have determined electrophoretic "fingerprints" of human erythrocytes to gain a deeper insight into the dynamical behavior of this particular surface. Also, increased understanding of the electrostatic and structural behavior of this well-characterized polyelectrolyte surface has resulted from applying the extended concept of charged layer electrophoresis.

Theory

We consider a particle whose radius is much larger than the Debye length κ^{-1}. The fixed surface charges are spatially distributed in a layer extending from the particle surface toward the bulk solution. This layer is considered to be uniform in the tangential direction. The thickness of the layer is assumed to be much smaller than the particle radius. Perpendicular to the surface m arbitrary distribution functions of m dissociable groups describe the potential spatial charge density of the dissociable sites $\rho_m(x)$. Here x denotes a coordinate axis perpendicular to the surface with the origin located at the particle surface. The m different dissociable sites are described by their respective pK_m and z_m values. z_m is +1 for a proton being released or, respectively, −1 for a proton generating a positively charged site by means of association. In the case of monovalent groups the actual fixed charge density ρ^m produced by the m-th group is given by

$$\rho^m = \frac{\rho_m(x)}{1 + 10^{z_m(pK_m - pH - (e_0\psi(x))/(kT\ln(10)))}} \quad (1)$$

Here $\psi(x)$ denotes the electric potential. e_0, k, and T are the elementary charge, the Boltzmann constant, and the absolute temperature, respectively. A corresponding relationship could be used to treat ion adsorption or association as well.

$\psi(x)$ is given by the solution of the linearized Poisson−Boltzmann equation

(21) Zhulina, E. B.; Borisov, O. V.; Birstein, T. M. *J. Phys.* **1991**, *II*, 512.
(22) Zhulina, E. B.; Borisov, O. V.; Birstein, T. M. *J. Phys.* **1992**, *II* (2), 63.
(23) Israëls, R.; Leermakers, F. A. M.; Fleer, G. J.; Zhulina, E. B. *Macromolecules* **1994**, *27*, 3249.
(24) Decher, G.; Hong, J.-D.; Schmitt, J. *Thin Solid Films* **1992**, *210/211*, 831.
(25) Lvov, Y.; Decher, G.; Möhwald, H. *Langmuir* **1993**, *9* (2), 481.
(26) Klitzing, R. v.; Möhwald, H. *Langmuir* **1995**, *11* (9), 3554.
(27) Lowak, K.; Helm, C. A. *Macromolecules* **1995**, *28* (8), 2912.
(28) Dahlgren, M. A. G.; Claesson, P. M.; Audebert, R. *J. Colloid Interface Sci.* **1994**, *166*, 343.
(29) Marlow, B. J.; Fairhurst, D.; Oja, T. *Abstracts, 60th Colloid and Surface Science Symposium*; Georgia Tech.: Atlanta, GA, 1986.
(30) Marlow, B. J.; Rowell, R. L. *Langmuir* **1990**, *6*, 1088.
(31) Heart, D. H.; Seaman, G. V. F. *J. Gen. Physiol.* **1960**, *43*, 635.
(32) Eylar, E. H.; Madoff, M. A.; Brody, O. V.; Oncley, J. L. *J. Biol. Chem.* **1962**, *237*, 1992.
(33) Cook, G. M. W.; Heard, D. H.; Seaman, G. V. F. *Nature* **1962**, *191*, 44.
(34) Donath, E.; Lerche, D. *Bioelectrochem. Bioenerg.* **1980**, *7*, 41.
(35) Benz, E. J. In *The Molecular Basis of Blood Diseases*; Stamatoyannopoulos, G., Nienhuis, A. W., Majerus, P. W., Varmus, H., Eds.; W. B. Saunders Comp.: Philadelphia, London, Toronto, Montreal, Sidney, Tokyo, 1994; p 257.
(36) Bäumler, H.; Halbhuber, K.-J.; Stibenz, J.; Lerche, D. *Biochim. Biophys. Acta* **1987**, *923*, 22.
(37) Eckstein, R. *Immunhämatologie und Transfusionsmedizin*; Gustav Fischer Verlag: Stuttgart, New York, 1990.
(38) Mollison, P. L. *Blood Transfusion in Clinical Medicine*; Blackwell Scientific Publications: Oxford, 1983.

$$\psi'' - \kappa^2\psi = -\frac{1}{\epsilon\epsilon_0}\sum_m \frac{\rho_m(x)}{1 + 10^{z_m(\mathrm{pK}_m - \mathrm{pH} - (e_0\psi(x))/(kT\ln(10)))}} = f[x,\psi(x)] \quad (2)$$

ϵ and ϵ_0 are the dielectric constant and the permittivity of a vacuum, respectively.

As we showed previously,[39] when the right-hand side of eq 2 does not depend on ψ, an analytical solution is possible. This was given in terms of Green function integrals over the net fixed charge density. This is not possible with eq 2 here. A further linearization of eq 2 is not meaningful either, since this would lead to a linear differential equation with variable but arbitrary coefficients. Therefore, an iterative numerical procedure was executed, starting from the analytical solution of eq 2, but with

$$f[x,\psi(x)] = -\frac{1}{\epsilon\epsilon_0}\sum_m \rho_m(x) \quad (3)$$

The calculated intermediate electric potential distribution was used to find, successively, the respective intermediate fixed charge density distributions. The procedure converged within a few cycles if the absolute electric potential was less than approximately 50 mV. Only in extreme cases were larger potentials calculated, because in the case of spatially distributed charges the Debye screening is more effective than that with surface charges. This justified the use of the linearized Poisson–Boltzmann equation.

When, as in the case of larger potentials, an oscillating behavior of the algorithm led to difficulties in the convergence, we introduced an electric potential averaged over two cycles, which was sufficient to obtain convergence.

When a pressure gradient, ∇p, is applied along the surface, the resulting hydrodynamic flow field, $v(x)$, is found by solving eq 4

$$\frac{\mathrm{d}^2v(x)}{\mathrm{d}x^2} = \frac{1}{\eta}\nabla p = \text{constant} \qquad x \geq \delta$$

$$\frac{\mathrm{d}^2v(x)}{\mathrm{d}x^2} - \alpha^2 v(x) = \frac{1}{\eta}\nabla p = \text{constant} \qquad x \leq \delta \quad (4)$$

Here $1/a$ is the characteristic length for flow penetration into the layer. δ denotes the charged layer thickness. η is the viscosity of the bulk electrolyte. The solution of eq 4, together with the electric potential distribution given by eq 2, can be used to find the electrophoretically effective charge density, $\sigma_{\mathrm{eff}} = \kappa\eta b$, where b stands for the electrophoretic mobility. A convenient way to calculate the effective charge density is the intermediate calculation of the streaming current density per unit length of the surface i. For more details the reader is referred to refs 9 and 40.

$$i = \int_0^\infty v(x)\, q(x)\, \mathrm{d}x \quad (5)$$

Here $q(x)$ is the charge density produced by the mobile small ions distributed according to $\psi(x)$.

Theoretical Results and Discussion

Let us start with the analysis of the simplest possible case of a spatial charge distribution of one single negatively charged site, homogeneously distributed in the charged layer, without flow penetration into the layer. We were interested in the dependence of σ_{eff} on both pH and ionic strength. For the sake of a convenient comparison with the experiments to be presented later on human erythrocytes, a net charge density of -0.022 C/m^2 of the negatively charged sites having a pK of 4 has been used throughout. In Figure 1 two different thicknesses of the layer were used. When the layer thickness was 5 nm (this value being larger than the respective Debye length for the three ionic strengths assumed), it is a characteristic feature that the electrophoretic effective charge is much less than the net surface charge density. The theoretical limit, in the case of surface charges being located in a plane, is -0.022. This value has been chosen as the origin of the ordinate axis. It can be seen that even the saturation value of σ_{eff}, far from the pK, does not approach the theoretical limit for plane surface charges. As expected, the difference between the theoretical limit for plane surface charges and the plateau values in the case of spatially distributed charges was reduced when the layer thickness decreased compared to the Debye length. This feature is obvious from the two curves calculated for a layer thickness of 0.5 nm. Here σ_{eff} approaches close to the theoretical limit if, as in the case of the 10 mM solution, the Debye length is 6 times larger than the layer thickness. It is worth emphasizing that it is the distribution of the surface charges in a layer which is responsible for the decrease of σ_{eff} with increasing ionic strength. The decrease of the electrophoretic mobility with increasing ionic strength induced by double-layer compression cannot be directly seen in Figure 1 because σ_{eff} is already standardized for this effect in the case of plane surface charges. An explanation for the remaining dependence of σ_{eff} on ionic strength is as follows. At small Debye lengths as compared to the layer thickness, most fixed charges are screened by counterions already within the layer and consequently do not contribute toward the electrophoretic mobility, provided the flow does not penetrate into the charged layer. This case resembles the situation of a shift of the plane of shear due to an adsorbed polymer layer. In the case of neutral polymers, electrophoresis has been employed to establish adsorption layer thicknesses.[42]

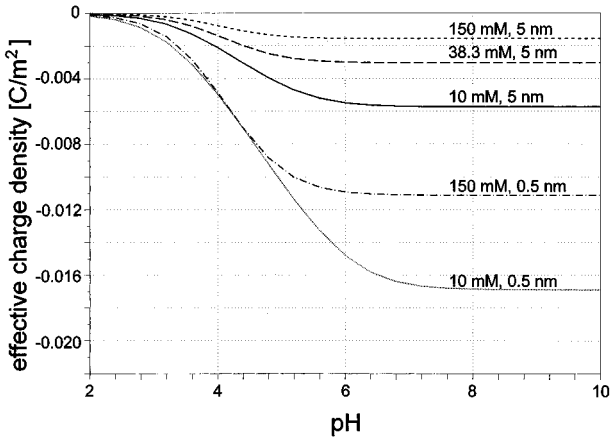

Figure 1. Theoretical plot of the effective charge density $\sigma_{\mathrm{eff}} = \eta\kappa b$ of a particle covered with a charged layer of different thicknesses as a function of pH and ionic strength. The spatial charge density in the layer was -0.022 C/m^2, pK = 4. No flow inside the layer.

We now explore, firstly, the influence of flow penetration into the layer and, secondly, the presence of an additional positively charged site. In Figure 2, for the sake of simplicity, it was assumed that both sides have the same uniform distribution, thus reducing the effect of two groups to a simple superposition of charge densities. In Figures 2 and 3 we focus on the effect of the hydrodynamic flow within the layer on the mobility, and subsequently the effect of the charge distribution itself is investigated.

(39) Pastushenko, V.; Donath, E. *Stud. Biophys.* **1976**, *56*, 7.
(40) Voigt, A.; Donath, E.; Kretschmar, G. *Colloids Surf.* **1990**, *47*, 23.
(41) Donath, E.; Pastushenko, V. *Bioelectrochem. Bioenerg. 7*, 31.
(42) Siffert, B.; Li, J. F. *Colloids Surf.* **1992**, *62*, 307.

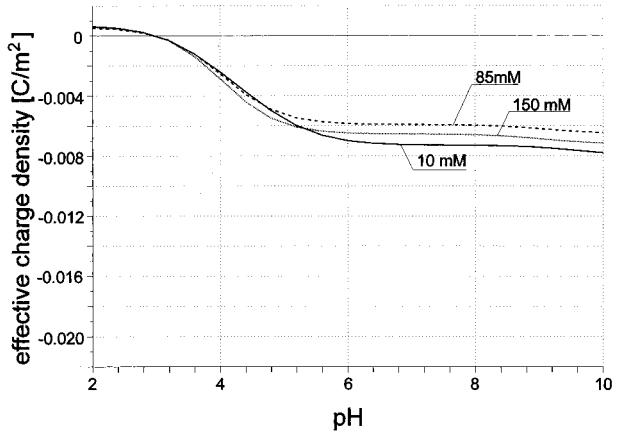

Figure 2. Theoretical plot of the effective charge density $\sigma_{eff} = \eta\kappa b$ of a particle covered with a charged layer as a function of pH with hydrodynamic flow penetration into the layer. Characteristic depth of flow penetration was 1 nm. Two charged groups present with p$K = 4$ and 9 and charge density $= -0.022$ and $+0.002$ C/m^2, respectively.

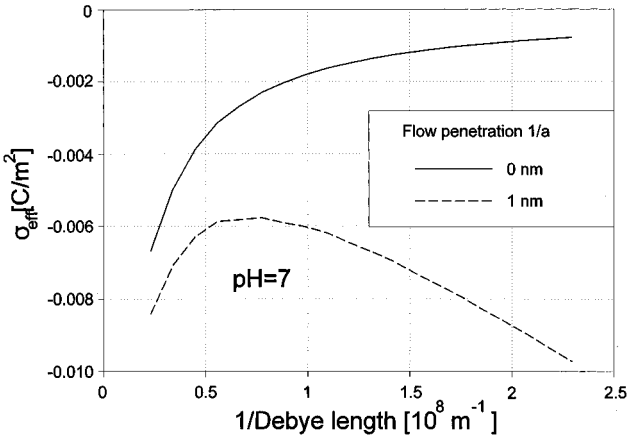

Figure 3. Comparison of the effective charge densities as a function of the ionic strength expressed in inverse Debye length in the absence and presence of hydrodynamic flow penetration.

With reference to Figure 2, consider a characteristic depth of flow penetration, $a^{-1} = \delta/5$. This represents a moderate flow penetrability. First of all, as a result of the assumed flow within the layer, the absolute value of σ_{eff} is increased as compared to the situation of no flow provided in Figure 1 (cf. in Figure 1 the curves for 5 nm layer thickness). The explanation is that an electroosmotic flow is now partially created within the layer, ensuring a more effective contribution from more deeply located fixed charges to the particle mobility. It is interesting to note that this increase of σ_{eff} is more pronounced for the larger ionic strength, leading to a nontrivial, nonmonotonous dependence of σ_{eff} on the Debye length, as demonstrated in Figure 3. The point of zero σ_{eff} (identical to the point of zero mobility) does not depend on ionic strength. This observation results from the underlying assumption of the identical, uniform distribution for both dissociable sites. The σ_{eff} curve for the case of 10 mM electrolyte intersects the other curves between the point of zero mobility and the plateau region. This is a result of the larger shift of the apparent pK in 10 mM electrolyte, as compared to higher ionic strengths, because here the absolute values of the electric potentials were higher.

While some of the aspects of Figures 1−3 have been known previously, the results presented in Figure 4 are new. Information regarding the fixed charge distribution itself can be obtained from the dependence of the zero point of mobility on ionic strength. We focus here on the

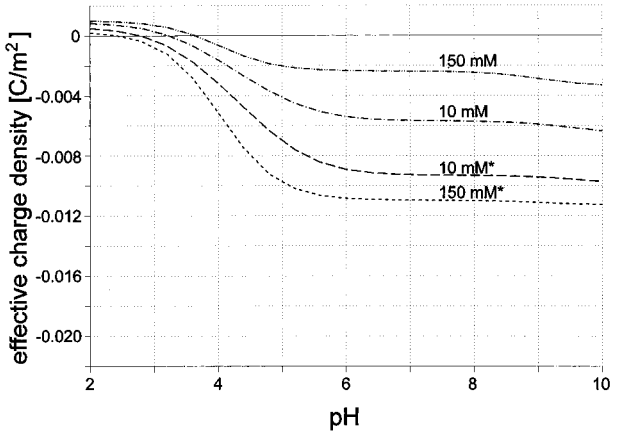

Figure 4. Theoretical plot of the effective charge density $\sigma_{eff} = \eta\kappa b$ as a function of pH, demonstrating the influence of linearly increasing or, respectively, decreasing toward the outside fixed charge distributions. The curves with the asterisks were calculated for linearly increasing toward the outside negative charge density of -0.022 C/m^2 together with decreasing toward the outside positive charge density of $+0.002$ C/m^2. The curves without asterisks describe the opposite case. In all curves the pK values were 4 and 9, respectively. No hydrodynamic flow penetration was present.

qualitative behavior of the point of mobility reversal (σ_{eff} reversal). Our analysis revealed that, in order to produce theoretically a dependence of the mobility reversal-point on the salt concentration, the charge distribution functions of the oppositely charged groups had to be different, independent of whether flow penetration was present or not. This is illustrated in Figure 4, where, in contrast to Figure 2, instead of homogeneous distributions for the charge densities, a linearly increasing site density distribution function together with one decreasing toward the outer edge of the hairy layer were assumed. The consequences were twofold. Firstly, this modified the plateau value of σ_{eff} far from the pK of the dominating group. The charged site which increased toward the bulk contributed more effectively to σ_{eff}. Secondly, this created the dependence of the zero σ_{eff} point on ionic strength. When, for example, the positive group increased in concentration toward the particle surface, while the distribution of the negative groups increased toward the bulk, the increasing accessibility of the positive groups upon decreasing ionic strength created a shift of the zero σ_{eff} point toward higher pH with decreasing ionic strength. Reversal of these two site distribution functions reversed this dependency. Flow penetrability weakened this effect because, as discussed in connection with Figure 2, penetration of flow increases the relative contribution of the deeper buried fixed charges to σ_{eff}. Figure 5 summarizes these results. Here the point of zero mobility is plotted as a function of the salt concentration expressed in terms of the inverse of the Debye length. Clearly, qualitatively different behavior of the zero point of mobility as a function of salt concentration is found when the charge distributions are reversed.

It should be realized that, in practice, there might be a variety of causes for different dissociable group distribution functions. For example, the actual molecular composition of the layer constituents could be responsible for site distribution asymmetry. On the other hand, pH- and ionic strength-dependent intra- as well as intermolecular electrostatic interactions may cause structural alterations of the charged surface layer, thus leading in turn to changes of the respective distribution functions. Another possibility is that, due to concentration-dependent adsorption, the charge of one particular site might depend

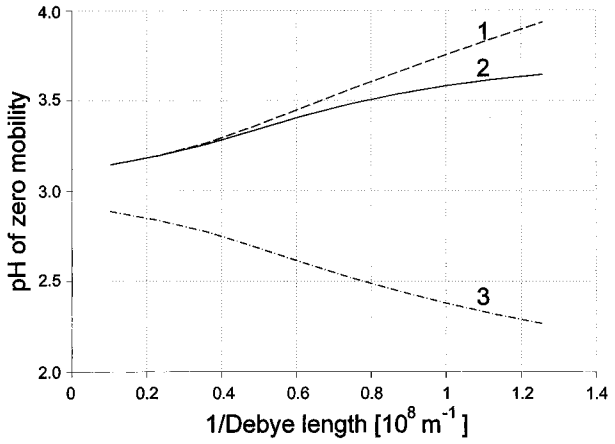

Figure 5. Zero mobility point as a function of ionic strength for the two cases of charge distribution. Curves 1 and 2 have the positive charges preferentially located toward the bulk (outside) while in curve 3 the negative charges increased toward the outside. In curve 2 additionally a flow penetration depth of 1 nm was taken into account.

on ionic strength. This would also lead to a shift of the zero mobility point as a function of ionic strength.

Another aspect worth mentioning is that in all cases σ_{eff} changed relatively slowly as a function of pH around the zero point of mobility in accordance with the assumed fixed charge density isotherm given in eq 1. Steep slopes, as observed in some experiments (see later) could not be produced with dissociation (and adsorption) equilibria alone. This, together with the mobility reversal dependence on ionic strength, is valuable new information which is necessary for the interpretation of experimental data. To our knowledge such information has not been previously utilized. In the next section we will demonstrate how these theoretical considerations can be applied to the often measured, but still not fully understood, particle surface of human red blood cells.

Materials and Methods

Materials. The sources of chemicals used for the particle electrophoretic experiments were as follows: neuraminidase (v. cholerae), Serva; methanesulfonic acid sodium salt (98%), Aldrich; and glutardialdehyde solution (25%), Merck.

Preparation of Erythrocytes. The source of cells for electrophoretic fingerprinting was fresh, human red blood cells, which had been washed three times in isotonic sodium chloride solution. Erythrocytes with reduced surface charge density were prepared by incubating red blood cells in 1 mL of NaCl solution (HK = 10%) with 0.25 and 5 μg of neuraminidase, respectively, for 60 min at 37 °C, followed by two subsequent washings with isotonic NaCl solution. Erythrocytes were fixed with glutardialdehyde as follows: 1.6 mL of a glutardialdehyde solution (25%) was slowly added to fresh red blood cells in 20 mL of phosphate-buffered saline until a final glutardialdehyde concentration of 2% was obtained. The mixture was stirred for 1 h at 25 °C before the erythrocytes were washed twice with phosphate-buffered saline.

Electrophoretic Measurements. Electrophoretic mobility (EPM)−pH curves and electrophoretic fingerprints were obtained using the ELECTROPHOR (HaSoTec) automated electrophoretic analyzer, which has been described in detail elsewhere.[43] Essentially, the instrumentation, which is based on a real-time image-processing system combined with a special tracking procedure, allows one to measure mean values of the electrophoretic mobility and fingerprints (simultaneous measurements of the electrophoretic mobility dependence on pH and conductance of the electrolyte over a wide range) in combination with a simultaneous particle discrimination based on other parameters, such as size, sedimentation rate, optical density, and shape of the individual particles. The mean mobility was reproducible to better than 2%. Electrophoretic measurements were made in sodium chloride solutions at concentrations in the range 10−150 mM. In one experiment chloride was replaced by sulfonate. The time needed to obtain the EPM−pH curves, at a given ion concentration, was less than 20 min.

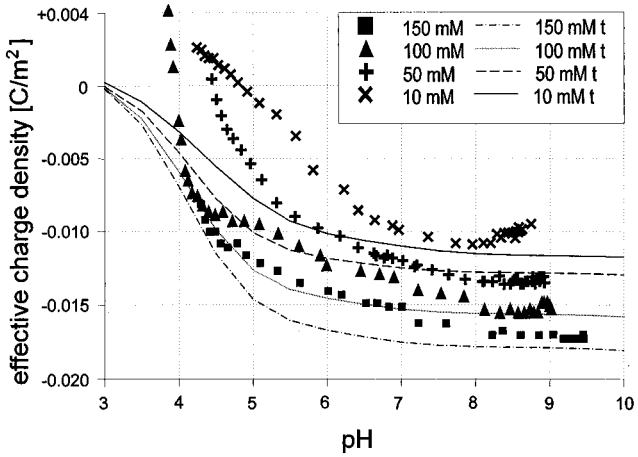

Figure 6. Effective charge density of washed human erythrocytes as a function of pH and ionic strength in NaCl.

Comparison of Human Erythrocyte Fingerprints. Evidence of Surface Structural Changes

It has been known for a long time that negatively charged sialic acid groups are the dominating charged groups of the human erythrocyte surface.[44,45] In addition, there are fixed charges provided by lipid head groups and amino acid side chains of the surface proteins. Thus, this surface has a polyelectrolyte nature. At pH values in the range 3.0−5.0 (depending on ionic strength) charge reversal takes place, which clearly demonstrates the presence of positive groups, as shown in Figure 6, where the experimentally determined electrophoretically effective charge density of washed human erythrocytes, as a function of the pH, for various electrolyte concentrations, is shown. Over a large range of pH the mobility is negative. It is widely accepted that these positive charges correspond to the amino groups of the surface glycoproteins. While the overwhelming majority of negative charges is composed of sialic acid residues, some carboxylic groups from the glycoprotein amino acid residues also contribute to the negative surface charge. There are approximately 500 000 glycoprotein molecules per cell.[46] 50−60% of these are glycophorin A.[47,48] Another major cell surface protein is band III, occurring in more than 10^6 copies per cell. The biochemical composition of the major glycoproteins of the erythrocyte surface is well established.[49−51] Glycophorin A has 16 oligosaccharide side chains, each of which carries two sialic acid residues. On the basis of this knowledge reasonable estimates regarding the net surface density of the various ionogenic groups can be made. In Table 1 we

(43) Grümmer, G.; Knippel, E.; Budde, A.; Brockmann, H.; Treichler, J. *Instrum. Sci. Technol.* **1995**, *23* (4), 265.

(44) Eylar, E. H.; Madoff, M. A.; Brody, O. V.; Oncley, J. L. *J. Biol. Chem.* **1962**, *237*, 1992.

(45) Luner, S. J.; Sturgeon, P.; Szklarek, D.; McQuiston, D. T. *Vox Sang.* **1975**, *29*, 440.

(46) Steck, T. L. *J. Cell Biol.* **1974**, *62*, 1.

(47) Fairbanks, G.; Steck, T. L.; Wallach, D. F. H. *Biochemistry* **1971**, *10* (13), 2606.

(48) Lutz, H. U.; Fehr, J. *J. Biol. Chem.* **1979**, *254* (22), 11177.

(49) Furthmayr, H.; Tomita, M.; Marchesi, V. T. *Biochem. Biophys. Res. Commun.* **1975**, *65* (1), 113.

(50) Kahane, I.; Furthmayr, H.; Marchesi, V. T. *Biochim. Biopys. Acta* **1976**, *426*, 464.

(51) Marchesi, V. T.; Furthmayr, H.; Tomita, M. *Hemat. Rev. Biochem.* **1976**, *45*, 677.

Table 1. Data of Surface Charge Distribution Used for Calculation of the Theoretical Curves in Figures 4−6[a]

charged group	p*K* value	charge density (C/m^2)	charge distribution
Asp, Glu	4.4	0.0054	uniform
			$1 - \chi^2$ after NaNase
			χ^2 after fixation
Lys	10	0.0012	uniform
		0.00012 after fixation	χ^2 after NaNase
Arg	12	0.0024	uniform
		0.0024 after fixation	χ^2 after NaNase
His	6.5	0.003	uniform
		0.0003 after fixation	χ^2 after NaNase
sialic acid	4	0.0198	$(\chi - 0.3)^2$
		0.01 after NaNase	$1 - \chi^2$ after NaNase
			$1/(1.2 - \chi)$ after fixation

[a] The charged layer thickness and the flow penetrability were 3.5 and 1 nm, respectively, throughout. χ denotes the distance from the particle surface in units of the layer thickness.

provide the estimated net surface charge density and the related p*K* values of the major groups.

To facilitate the discussion of the electrophoretic mobility behavior of the erythrocytes, we have constructed theoretical plots based on the parameters provided in Table 1. As free parameters the charge distribution, the glycocalyx thickness, and the flow penetration depth into the layer may be used. To adjust the theoretical curves to the experimental data, the most important parameter to be chosen is the glycocalyx thickness, since this determines, together with the given net charge (Table 1), the spatial charge density (eq 1). It was not possible to freely choose the distribution functions of the groups. As explained below they are in effect defined by the mobility reversal dependency on pH.

A characteristic feature of the erythrocyte mobility behavior is that, in the range of neutral and high pH, the absolute value of the effective charge density σ_{eff} increases with increasing ionic strength. This change is monotonous between 10 and 150 mM salt concentration. It is clear that this increase cannot be explained purely in terms of an increase of the amount of negative surface charges. As the theoretical curves show, this effect can easily be explained by the spatial arrangement of the fixed charges within the layer. Assuming a characteristic flow penetration depth of 1 nm into the 3.5 nm thick layer, we could theoretically reproduce σ_{eff} and its moderate increase at high pH. The observed layer thickness estimate of 3.5 nm is in good agreement with electron microscopy data[52] and values obtained by other groups.[8] The charge distribution functions provided in Table 1 have been constructed on the basis of literature values and from our own experimental data, as explained below. Important in this respect is the bimodal distribution of the sialic acid groups for the control. This is consistent with protein structure predictions suggesting sialic acid arangement in two layers.[53,54] It is also possible to explain the increase of the effective charge density upon an increase in ionic strength by a glycocalyx thickness change as a function of the salt concentration, resulting in a layer expansion upon a decrease in ionic strength.[7] This is equivalent to a decrease of the absolute value of the spatial charge density. It is generally not possible to easily distinguish between layer expansion and flow penetrability effects, since layer expansion is naturally associated with increased flow penetration as well.

It is interesting to note in Figure 6 that, in the range of decreased protonation of the amino groups (pH > 8) at low ionic strengths, a well pronounced decrease of the absolute value of σ_{eff} (of the order of 20%) occurs. This contradicts what one would have expected from the gradual increase of the negative charge density in this region, due to decreased protonization, which is seen at electrolyte concentrations of 100 and 150 mM, respectively. Clearly, the difference between the theoretical plots and the experiments increases at low ionic strength and high pH. An explanation for this apparent decrease of the mobility might be that a surface layer expansion of approximately 20% occurs, resulting in a decrease of the spatial density of the negative charges. It is probable that, at not too high pH values, some of the positive charges stabilized the layer by means of attractive electrostatic interaction with the negative charges. The gradual loss of the positive charges due to proton release with rising pH could thus result in a swelling of the surface layer created by the increased electrostatic repulsion. This hypothetical repulsive interaction should be of long range, since it became pronounced only when the Debye length increased above 1.5 nm (below 50 mM). This is close to the characteristic distance between the negative charges in the surface layer.[34]

Let us now have a closer look at the range of the electrophoretically effective charge reversal. A shift of the point of zero mobility to lower pH with increasing ionic strength is evident. The shift was of the order of 1 pH unit when the ionic strength was increased from 10 to 150 mM. The theoretical plots qualitatively predicted this shift. This could only be achieved by assuming a preferential occurrence of the negative groups in the outer region of the glycocalyx. The experimental points of zero mobility, however, were seen at higher pH. One possibility to account for the quantitative discrepancy between the theoretical and the experimental curves would be to assume unreasonably high p*K* values, of the order of 5−6, for the sialic acid groups. Another aspect in this connection is that the slope, especially at high ionic strengths, is relatively steep as compared with those of the theoretical curves. The sharp "bend" in the 100 mM experimental curve is very instructive. Such a sharp increase of the apparent charge density cannot be explained by means of more gradual dissociation equilibria. These findings point to an increasing influence of the positive charges on the apparent charge density at low pH, as compared to high pH, where the mobility does not increase as much as expected due to the decreased protonization. To test this assumption, it would useful to measure the mobility in the range of very low pH where a saturation of σ_{eff} is expected. Unfortunately, it is not possible to reach this region. The cells start increasingly to hemolyze below pH = 3.5. But, even so, it is clear that the possible plateau value of σ_{eff} in the low-pH region is much too high given the small charge density of the positive charges inferred from the behavior at high pH. These discrepancies between the theoretical predictions and the experiments in the range of the zero mobility region therefore required a new explanation. Obviously, structural alteration of the surface layer leading to a more condensed layer, has to be taken into account to explain the mobility behavior near the zero mobility point. This would produce an apparent increase of the positive charge density. Also, it cannot be excluded that the positive groups become more exposed. This may be the result of the diminished electrostatic repulsion between the sialic acid groups due to a smaller degree of dissociation.

(52) Skutelsky, E.; Danon, D.; Wilchek, M.; Bayer, A. *J. Ultrastruct. Res.* **1977**, *61*, 325.
(53) Halbhuber, K.-J.; Gliesing, M.; Stibenz, D.; Makovitzky, J. *Histochemistry* **1984**, *81*, 187.
(54) Bäumler, H.; Halbhuber, K.-J.; Stibenz, D.; Lerche, D. *Biochim. Biophys. Acta* **1987**, *923*, 22.

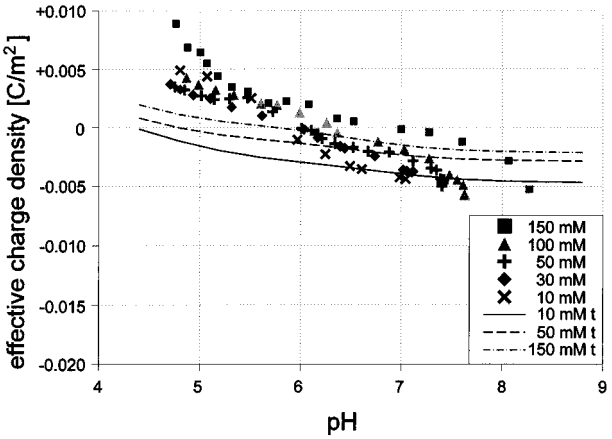

Figure 7. Effective charge density of neuraminidase-treated human erythrocytes as a function of pH and ionic strength.

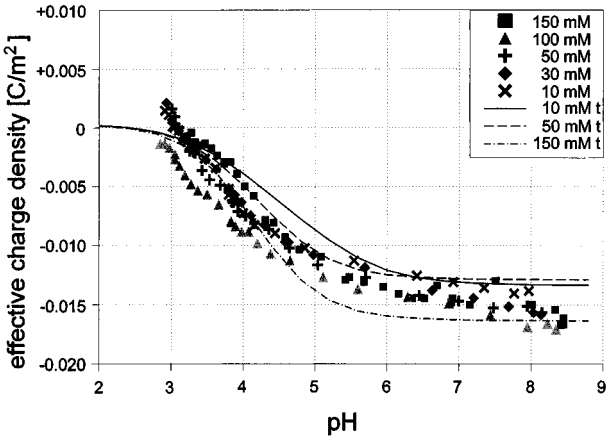

Figure 8. Effective charge density of glutardialdehyde-fixed human erythrocytes as a function of pH and ionic strength.

It is worth remembering that the theoretical pH shift of the zero mobility point is the result of the preferential occurrence of the negative charges at the outer regions of the surface layer. A bimodal distribution of the sialic acid groups is nessecary to explain the experimental observed pH shift. Alternative explanations of this shift would be the adsorption of anions to neutral sites and the association of anions to the positive groups. To discriminate between the density distribution effect on the pH shift of the zero mobility point and the association/dissociation mechanism, we replaced chloride by sulfonate. No influence on the mobility behavior was found, thus making the idea of adsorption or association less attractive. It should be realized that the assumed structural alterations may additionally modify the pH shift.

To further test the hypothesis of electrostatically induced structural alterations of the charged layer, the following (conclusive) experiment is possible. By means of neuraminidase treatment one can gradually remove sialic acid sites.[50,55] The result can be seen in Figure 7, where the charge has been removed to approximately half of its original value. The result is conclusive. First, the point of zero σ_{eff} has significantly shifted toward higher pH, reflecting the increased relative contribution of positive charges to the net effect. Even more decisive is the reversal of the order of the pH shift as a function of ionic strength. This reversal of the order occurred gradually. At smaller degrees of charge removal there were conditions where almost all the curves coincided and intersected the abscissa at the same pH value. Obviously, the removal of the negative charges occurred preferentially in the outer regions of the charged layer, thus making the surface more positive at high ionic strengths, where mainly the fixed charges in the outer regions of the layer determine σ_{eff}. The theoretical curves reproduce well the pH shift of the zero point of mobility when the remaining positive charges are preferentially distributed toward the outer border of the layer. This again emphasizes the importance of the charge distribution asymmetry for the zero mobility point. The fact that neuraminidase preferentially removes sialic acid groups in the outer region of the glycocalyx is consistent with biochemical findings. It has been shown that, even when the electrophoretic accessible sialic acid is almost completely removed, still $^1/_5$ of the original sialic acid remains biochemically detectable[56] and, hence, is probably located beneath the charged surface layer. As in the case of the control, at low pH the theoretical results are significantly smaller than the experimental data. The same reasoning as above, based on layer compression, has to be applied to explain this decrepancy. Obviously, in the region of low pH the apparent density of the positive charges is larger than that at high pH. This can only be explained by an increased exposure of the positive groups, due to structural rearrangements in the glycocalyx, upon pH reduction. The alternative possibility of the assumption of positive groups with such a low p*K* below 5.5 is highly unlikely.

The tendency of the absolute value of the effective charge density to increase above neutral pH is also remarkable. An explanation could be that, in the range of neutral pH and below, the surface structure is partly determined by attractive electrostatic interaction corresponding to the close proximity of negative and positive sites. This would cause a partial mutual compensation of fixed charges. Deprotonization of the amino groups releases the negative sites, thus producing a pronounced increase of the negative σ_{eff}.

The importance of the positive charges for the electrostatic structure of the surface layer, which to date has been overlooked, was further demonstrated when a glutaraldehyde treatment was performed to remove the majority of positive sites, by means of the reaction of the aldehyde carbonyl groups with the amino and imino groups of the positively charged amino acids. Earlier experiments had led to the erroneous conclusion that the positive charges do not contribute to the mobility.[57] While indeed the mobility under physiological conditions almost did not change in these studies, it is clearly seen that the mobility around the zero point is affected strongly by the aldehyde treatment. We have reproduced these earlier results which correspond to a removal of the ionic strength dependence of the zero point of mobility together with a shift toward lower pH.[57] Our experimental data are given in Figure 8. As expected, the point of zero σ_{eff} is shifted to lower pH values, together with an overall increase of σ_{eff} at ionic strengths below 150 mM. Within the range of the experimental error, the point of zero σ_{eff} does not depend on the ionic strength. This demonstrates that indeed the different distribution functions of the positive and negative groups are responsible for the previously observed pH shift. In support of this are the absence of the distinct effective charge decrease at high pH and the much smaller difference between the effective charge densities obtained at 10 and 150 mM, as compared to the case for native cells (Figure 6), which was interpreted

(55) Schauer, R.; Corfield, A. P.; Wember, M.; Danon, D. *Hoppe-Seyler's Z. Physiol. Chem.* **1975**, *356*, 1727.

(56) Luner, S. J.; Sturgeon, P.; Szklarek, D.; McQuiston, D. T. *Vox Sang.* **1975**, *28*, 184.

(57) Heard, D. H.; Seaman, G. V. F. *Biochim. Biophys. Acta* **1961**, *53*, 366.

above as being a consequence of the ionic strength-modulated electrostatic interaction. The absence of these changes in the case of the glutaraldehyde-fixed cells once more underlines the importance of the positive charges for the surface layer structure. The slopes near zero σ_{eff} are more gradual, indicating the absence of sharp structural alterations, which is again a consequence of the largely reduced presence of positive groups. It is also worth mentioning that glutaraldehyde-induced cross-linking could have partially removed the capability of the glycoproteins to demonstrate structural alterations responsible for the features of the electrophoretic behavior discussed above.[58] The discrepancy between the theoretical curves and the experimental data below the zero point of mobility is a consequence of the theoretically assumed 90% reduction in the number of positive groups. Another point to note is that the zero mobility point, compared approximately to pH 3, indeed demonstrates that the sialic acid p*K* was close to pH 3. Thus, the discrepancy of the zero mobility region between the experimental and theoretical curves in the case of washed and neuraminidase-treated cells can indeed not be explained by means of assuming a higher p*K* of the sialic acid. Even our assumption of a p*K* of 4 seems to be relatively high.

Summarizing the above discussion, we would like to make the conclusion that, by means of a comprehensive interpretation of electrophoretic fingerprints, taking into account the charged layer concept of electrophoresis, an improved qualitative understanding of the erythrocyte mobility behavior is now possible. A major conclusion is that throughout electrostatically modulated surface structural alterations play a major role in explaining the mobility behavior. That ionic strength dependent conformational changes of the surface glycoproteins indeed take place has been found, also by means of biochemical and aqueous two-phase partition methods.[59,60]

Without assuming flow penetration of approximately 1 nm into the layer, we were not able to quantitatively describe the mobility behavior of the layer. Thus, the picture of a relatively loose structure of the surface layer of the erythrocytes at least in the outer regions is quite probable. The theoretical and experimental demonstration of the zero mobility dependence on ionic strength being a result of asymmetry of the fixed charge distribution seems to us a valuable new aspect of electrophoretic investigations. It might be useful for the interpretation of various polyelectrolyte surfaces in colloid chemistry as well.

With respect to the theoretical plots, we would like to underline that it was not our primary aim to obtain good fits of the experimental data but to provide a theoretical background for the interpretation of the experimental data. Therefore, we did not attempt to include ionic strength-dependent structural alterations in the theoretical calculations. We changed neither the layer thickness nor the flow penetrability independent of the treatment performed. Only the charge distributions had to be changed in order to qualitatively describe the zero mobility dependence on ionic strengths. Given the large number of free parameters, especially the freedom in the choice of assuming charge distribution functions and structural changes upon ionic strengths, it would have been, in principle, possible to obtain complete coincidence between theory and experiment. Yet, this has to be done with great care not to be too speculative and not to violate basic physicochemical principles.

We are aware that there are still many limitations of our considerations. Despite the better quantitative theoretical understanding achieved above, it would have been still too speculative to attempt quantitatively better fits of the experimental data. It is worth noting that, in reality, the p*K* values of the individual surface charge generating groups may not be a constant but may depend on the local chemical environment.

It is also clear that, at low ionic strength, the validity of the linearization of the Poisson−Boltzmann equation is not ensured. This restricted us to red cell mobility data above 10 mM, where the corresponding electric potentials are at most of the order of 30 mV. For the same reason the surface conductivity has not been included in this linear theory. It will become a major correction in the range of surface charge density−ionic strength where the linear hairy layer electrophoretic approach presented here is not applicable. A combination of recent surface conductivity treatments[61−63] with "hairy layer" particle electrophoresis is currently under progress. Also quite possible are a change of the dielectric constant and associated effects generating an altered small ion distribution between the layer and the bulk. Clearly, for a much broader application of electrokinetics to hairy particles a nonlinear theory including the surface conductivity effect upon mobility is required. Such work, extending the range of applicability of hairy layer electrophoresis, is currently in progress. Unfortunately, this extension requires much more sophisticated numerical procedures. A further step should be the generalization of this concept to small particles.

Nevertheless, despite these shortcomings the sensitivity of electrophoresis to the charged layer properties in the short-nanometer range has already been shown to be very valuable for a better understanding of interfacial electrostatics. We hope that this work will lead to a broader application and deeper interpretation of electrophoresis than in the past.

Acknowledgment. This work was supported by grants from the Deutsche Forschungsgesellschaft: Do 410/2−1, Kn 385/1-2, and Ba 1545/1-1. We are particularly indebted to stimulating discussions with S. S. Dukhin, H. Möhwald, and B. Vincent.

LA960204M

(58) Geyer, G. *Bas. Appl. Histochem.* **1980**, *24*, 3.
(59) Zaslavsky, B. Y.; Miheeva, L. M.; Rogozhin, S. V.; Borsova, L. V.; Kosinez, G. I. *Biochim. Biophys. Acta* **1980**, *597*, 53.
(60) Jenkins, R. E.; Tanner, M. J. A. *Biochem. J.* **1977**, *161*, 131.
(61) Kijlstra, J.; Van Leeuwen, H. P.; Lyklema, J. *J. Chem. Soc., Faraday Trans.* **1992**, *88*, 3441.
(62) Hidalgo-Alvarez, R.; Moleon, J. A.; De las Nievas, F. J.; Bijsterbosch, B. H. *J. Colloid Interface Sci.* **1992**, *149*, 23.
(63) Van der Wal, A. Electrochemical Characterization of the Bacterial Cell Surface. Thesis, Landbouwuniversiteit Wageningen, 1996.